Research Square

Preprints are preliminary reports that have not undergone peer review.
They should not be considered conclusive, used to inform clinical practice,
or referenced by the media as validated information.

Using a stochastic phenology model to assess the potential northern range limit of Conotrachelus nenuphar in Europe under current and future climate

Juha Tuomola

juha.tuomola@ruokavirasto.fi

Finnish Food Authority: Ruokavirasto https://orcid.org/0000-0001-5620-8693

Mariela Marinova-Todorova

Finnish Food Authority: Ruokavirasto

Stafva Lindström

Finnish Food Authority: Ruokavirasto

Leonard Owuraku Opare

Finnish Food Authority: Ruokavirasto

Research Article

Keywords: Climate, Plant health, Quarantine pest, Risk assessment, Risk management

Posted Date: June 26th, 2026

DOI: https://doi.org/10.21203/rs.3.rs-10042133/v1

License: This work is licensed under a Creative Commons Attribution 4.0 International License.
Read Full License

Research article

Using a stochastic phenology model to assess the potential northern range limit of *Conotrachelus nenuphar* in Europe under current and future climate

Juha Tuomola[1,*], Mariela Marinova-Todorova[1], Stafva Lindström[1,2], Leonard Opare[1]

[1]Finnish Food Authority, Mustialankatu 3, FI-00790 Helsinki, Finland. Email: juha.tuomola@ruokavirasto.fi
[2]University of Helsinki, Faculty of Agriculture and Forestry, Department of Microbiology, Helsinki, Finland

*Corresponding author

Juha Tuomola ORCID: 0000-0001-5620-8693
Mariela Marinova-Todorova ORCID: 0009-0006-1486-7686
Stafva Lindström ORCID: 0000-0002-2863-940X
Leonard Opare ORCID: 0000-0003-4695-2675

Acknowledgements

We thank the Finnish Government for funding the Postdoctoral Programme for Research Institutes in Finland, which supported this research. We acknowledge the World Climate Research Programme, which, through its Working Group on Coupled Modelling, coordinated and promoted CMIP6. We thank the climate modelling groups for producing and making available their model output, the Earth System Grid Federation (ESGF) for archiving the data and providing access, and the multiple funding agencies who support CMIP6 and ESGF. We acknowledge the Copernicus Climate Change Service for providing access to ERA5 climate data and the Pan European Phenological Database PEP725 and its partner organizations for providing access to phenological observations used in this study.

Abstract

Conotrachelus nenuphar is a major pest of several stone and pome fruits in North America. Although currently absent from Europe, it is classified as a priority pest under European Union (EU) plant health legislation, requiring official surveillance in areas where establishment and spread are possible. To support EU risk management, we assessed the potential northern range limit of *C. nenuphar* in Europe under current climate (2006–2025) and mid-21st-century projections (2041–2060) under SSP2-4.5. This was done using a stochastic phenology model that simulates temperature-dependent developmental steps of the northern strain of *C. nenuphar* on sour cherry and evaluates whether its life cycle can be completed within one calendar year. Thermal requirements are represented as probability distributions derived from published empirical studies, and each stochastic iteration simulates the development of one individual sampled from these distributions. We ran the model across central and northern Europe using 500 stochastic iterations and summarized the results using the mean life cycle completion proportion and the proportion of successful years. Under current climate, central Europe appears thermally suitable for the establishment of the northern strain of *C. nenuphar*. In contrast, Finland, most of Ireland and Sweden, and parts of the Baltic region were insufficiently warm, suggesting a very low likelihood of establishment. Future projections indicated increased thermal suitability in these regions, but not to levels suggesting likely establishment in the northernmost EU. These results support evaluation of where official surveillance for *C. nenuphar* in the EU is warranted.

Keywords

Climate; Plant health; Quarantine pest; Risk assessment; Risk management

Introduction

Conotrachelus nenuphar Herbst (Coleoptera: Curculionidae), commonly known as the plum curculio, is a weevil native to eastern North America and a major pest of several stone and pome fruit species (Quaintance and Jenne 1912; Chapman 1938; Lampasona et al. 2020). Although its current distribution is limited to its native range, *C. nenuphar* is considered a significant potential threat to plant health in the European Union (EU) and is consequently classified as a priority pest under EU plant health legislation (European Commission 2019). In this context, priority pests are Union quarantine pests whose potential economic, environmental, or social impacts are regarded as the most severe (European Parliament and Council of the European Union 2016; European Commission 2019).

For each priority pest, all EU Member States are required to implement strict surveillance measures, including annual surveys and contingency planning, aimed at preventing introduction and facilitating early detection of possible outbreaks (European Parliament and Council of the European Union 2016). However, these obligations do not apply if it can be demonstrated unequivocally that the priority pest cannot establish or spread in a Member State due to unsuitable ecoclimatic conditions or the absence of host plants (European Parliament and Council of the European Union 2016). Brief EU level assessments suggest that climatic conditions in Europe should not limit the establishment of *C. nenuphar*, and that the pest could establish wherever suitable host plants are present (EFSA 2018a, 2019, 2025).

However, climatic suitability for *C. nenuphar* in the northern EU is not necessarily so self-evident as brief assessments may suggest. The pest has two distinct strains, a southern strain with two or more generations per year with a facultative diapause, and a northern strain with only one generation per year and an obligate winter diapause (Chapman 1938; Smith and Salkeld 1964). The northern strain occurs in the northern United States and southern Canada, where winters are colder than those in Europe, including northern Europe, but where summers are warmer than in regions such as Scandinavia and the Baltic countries. Because *C. nenuphar* overwinters exclusively as an adult (Quaintance and Jenne 1912), its entire life cycle must be completed within one growing season. Armstrong (1958), however, showed that some adults can survive well beyond one season under optimum insectary conditions, indicating a limited potential for demographic carry-over between years. At the same time, Armstrong (1958) also concluded that adult longevity under field conditions was considerably lower than this physiological potential. Thus, summer temperatures are critical for survival and reproduction of *C. nenuphar*, and establishment is generally only possible in areas where developmental requirements can be met within a single season.

An assessment conducted in Sweden indicates that summer temperatures allow completion of the *C. nenuphar* life cycle in a single season only in the southern part of the country (Boberg and Björklund 2020b). However, Boberg and Björklund (2020b) concluded that due to rather limited data their assessment is

uncertain, and further analysis is required to more precisely identify the area where establishment is likely. Consequently, to ensure efficient allocation of official plant health resources in the EU, a more detailed assessment is needed to determine where temperatures in northern Europe are sufficient to support completion of the *C. nenuphar* life cycle.

Accumulated growing degree days (GDD) are frequently used in pest risk assessments to model temperature-dependent development of pest insects and evaluate whether climatic conditions permit completion of development within a reasonable timeframe (Venette et al. 2010; Eyre et al. 2012; Kriticos et al. 2024; Rosace et al. 2024). These GDD values can be easily derived from phenological observations and are straightforward to apply. However, their use often involves simplifications, such as assuming that the development of all life stages of insects can be represented by a single developmental threshold and a single overall accumulated GDD requirement, without accounting for intraspecific variation (e.g. Baker 2002; Magarey et al. 2011; Eyre et al. 2012; Kriticos et al. 2015; EFSA 2017, 2018b; Wakie et al. 2018; Burne 2019; EPPO 2024; Tuomola and Hannunen 2024). The developmental thresholds differ among insect life stages and incorporating these stage-specific thresholds would improve the accuracy of the assessments. Likewise, the accumulated GDD required to complete each developmental stage varies among individuals within a population. If empirical GDD data are normally distributed, the mean value represents the point at which half of the individuals fall above and half below the requirement. Consequently, relying solely on mean values may lead to an incomplete understanding of establishment potential. A more robust assessment should therefore incorporate intraspecific variation when drawing conclusions about the likelihood of establishment.

The aim of this study was to develop a stochastic phenology model that incorporates intraspecific variation in the temperature-dependent development across all life stages of the northern strain of *C. nenuphar*, using sour cherry (*Prunus cerasus* L.) as the host plant. The model simulates the accumulated thermal requirements of the northern strain, expressed primarily as GDD but also as number of days with mean temperature above a threshold, and is used to assess the potential northern range limit of the strain in Europe under current and future climatic conditions, based on whether temperatures are sufficient to support completion of its life cycle in a single season. Sour cherry was selected as a host in the modelling framework because GDD estimates for larval development of the northern strain are available, it is widely distributed across Europe, and development of *C. nenuphar* on this host is among the fastest reported (Selby and Whalon 2014), making it a suitable case study for exploring the potential range of the pest. Consequently, if *C. nenuphar* is unable to complete its life cycle on sour cherry, it is even less likely to do so on less suitable hosts. The northern strain was chosen for this study because it is adapted to the colder regions of North America and therefore is the strain most likely to be able to establish in the northern parts of Europe.

Methods

The stochastic phenology model was developed to estimate the timing of four sequential developmental steps of the northern strain of *C. nenuphar* on sour cherry using daily temperature data from the start of a calendar year (1 January) (Table 1). Each developmental step corresponds to a specific stage in the pest's life cycle. The first step describes the spring emergence of overwintered adults and estimates the timing of the onset of oviposition O_t. The second step describes egg hatching and larval development within the fruit and estimates the date at which mature larvae emerge the fruit L_t. The third step covers pupation in the soil and estimates the timing of emergence of the new-generation adults A_t. The fourth and final step describes the accumulation of sufficient reserves for overwintering and estimates the date at which individuals complete the annual life cycle and reach overwintering readiness F_t.

The purpose of the model is to determine whether all four developmental steps can be completed within a single calendar year under given climatic conditions. In addition, the model can be used to estimate the timing of the individual development steps (O_t, L_t, A_t, F_t) of the pest on sour cherry, but those features are not demonstrated further in this study.

The underlying thermal requirements for completing each step are represented as probability distributions, which capture the intraspecific variability documented in previously published empirical studies. The model operates as a stochastic simulation, where each run represents the temperature-dependent development of an individual insect randomly sampled from the defined probability distributions. The simulations are implemented in R (R Core Team 2024), and the full script used to define the distributions and perform the simulations is available at Zenodo (https://doi.org/10.5281/zenodo.20541446).

We used a large language model (Microsoft Copilot) to support parts of the data analysis workflow, specifically to suggest candidate probability distributions for the response variables and to generate draft versions of R scripts for model implementation. These outputs were checked, further edited, and validated by the authors, who take full responsibility for all analytical decisions and the final code.

The biological rationale for each of the four developmental steps is described in detail in the following sections.

Table 1. Parameters and derived variables included in the stochastic phenology model for the northern strain of *C. nenuphar* on sour cherry.

Parameter	Description	Derived variable	Source of the data

D_{imm}	Accumulated $GDD_{6.1}$ required by *C. nenuphar* for spring emergence and movement to host trees.	Simulated calendar date of adult immigration into host trees I_t, and eventually the calendar date of realized oviposition date O_t.	Piñero and Prokopy (2006)
D_{pf}	Accumulated GDD_4 required by sour cherry to reach petal fall stage (BBCH 69).	Simulated calendar date of petal fall of sour cherry P_t.	Zavalloni et al. (2006); Templ et al. (2018)
D_{ovi}	Accumulated GDD_{10} required by *C. nenuphar* to oviposit after the petal fall.	Simulated calendar date of oviposition-ready date O_{tr}, and the calendar date of realized oviposition date O_t.	Reissig et al. (1998)
D_{lar}	Accumulated GDD (11.1 °C and 35 °C as the lower and upper development thresholds) required for egg hatching and larval development on sour cherry fruits.	Simulated calendar date of emergence of mature larvae from sour cherry fruits L_t.	Selby and Whalon (2014)
D_{pupa}	Accumulated $GDD_{8.7}$ required by *C. nenuphar* for the pupal development and emergence of adults from soil.	Simulated calendar date of emergence of the new generation adults from soil A_t.	Selby and Whalon (2014)
D_{fall}	Number of days (with mean temperature ≥ 13 °C) required for post-emergence feeding and accumulation of reserves required for successful overwintering.	Simulated calendar date of completion of the life cycle and the onset of overwintering readiness F_t.	Spurgeon and Raulston 2006; Spurgeon et al. (2018)

Step 1: From overwintering to oviposition

In the early spring the overwintered adults of *C. nenuphar* emerge from the soil and fly to the trees where they mate and feed on the leaves, twigs, buds, flowers, and developing fruits (Crandall 1905; Chapman 1938; Racette et al. 1992). The females start laying eggs once the fruitlets are available, which occurs around the petal fall stage (when about 90% of the petals have fallen exposing the developing fruitlets) (Reissig et al. 1998). The oviposition period extends for several weeks, during which a female may lay several hundred eggs (Crandall 1905; Whitcomb 1929; Chapman 1938).

Both the pre-oviposition (emergence, immigration into the host trees and mating) and the oviposition period of *C. nenuphar* are strongly temperature-dependent (Whitcomb 1932; Racette et al. 1992) and the GDD requirements for these phases have been quantified for the northern strain of the species (Reissig et al. 1998; Hoffmann et al. 2004; Piñero and Prokopy 2006). Similarly, the phenological development of host trees is strongly influenced by the temperature and the accumulated GDD required to the petal fall stage or analogous BBCH stage (Biologische Bundesanstalt, Bundessortenamt und Chemische Industrie) (BBCH 69)

(Meier 2018) have been recorded for many tree species and cultivars in the Rosaceae family (e.g. Zavalloni et al. 2006; Singh and Bhatia 2011; Hochmaier 2014; Chaves et al. 2017; Templ et al. 2018; Verma et al. 2023).

Date of immigration

Piñero and Prokopy (2006) monitored the immigration of the northern strain of *C. nenuphar* into an apple orchard over six years and reported the annual accumulated GDD values corresponding to the first capture, and for 50th and 80th percentiles of cumulative captures for each year using a temperature threshold of 6.1 °C. Based on this data we fit a single probability distribution of the accumulated $GDD_{6.1}$ required for spring emergence of *C. nenuphar* and movement to host trees D_{imm} (Figure 1a). This was done by fitting a lognormal distribution by matching the observed quantiles to the corresponding cumulative distribution values using a weighted least-squares procedure. Weights corresponded to the annual capture counts. The final parameter estimates were obtained by minimizing the weighted squared differences between the observed cumulative probabilities (first capture, 50th and 80th percentile) and those predicted by the lognormal distribution. The distribution is used in the model to simulate the immigration date I_t for individual insects.

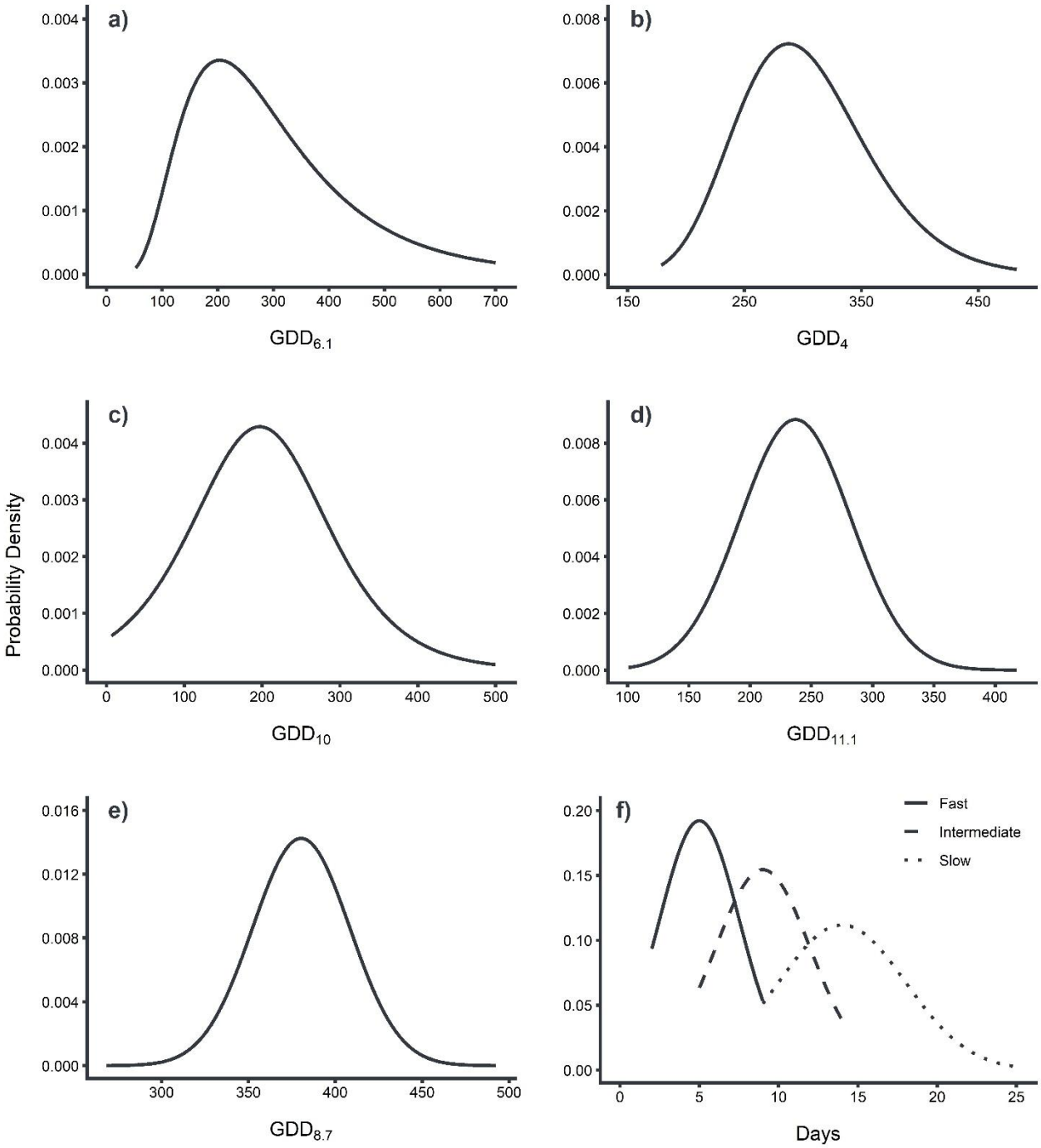


Figure 1. Fitted probability distributions used in the stochastic phenology model for the northern strain of *C. nenuphar* on sour cherry. (a) Accumulated $GDD_{6.1}$ required for spring emergence and movement of overwintered adults to host trees (D_{imm}). (b) Accumulated GDD_4 required for sour cherry to reach the petal fall stage (D_{pf}). (c) Accumulated GDD_{10} required by *C. nenuphar* for oviposition after petal fall (D_{ovi}). (d) Accumulated $GDD_{11.1}$ required for egg hatching and larval development on sour cherry fruits (D_{lar}), fitted to a synthetic population used to sample the 500 stochastic values applied in this study. (e) Accumulated $GDD_{8.7}$ required for pupal development and emergence of adults from soil (D_{pupa}). (f) Number of days with mean temperature ≥ 13 °C required for post-emergence feeding and accumulation of reserves for successful overwintering (D_{fall}), shown for the "fast", "intermediate" and "slow" scenarios.

Date of petal fall

Because oviposition can only occur once fruitlets are available, the model also requires an estimate of the timing of petal fall of sour cherry P_t. To capture potential variability in the timing of petal fall among different sour cherry cultivars, we defined a probability distribution for the accumulated GDD required for petal fall D_{pf} using data from the Pan European Phenological database (PEP725) for Germany (Templ et al. 2018; PEP725 Pan European Phenology Data 2026). This dataset includes phenological observations of sour cherry from 1951 to 2015 across more than 6,000 locations. For the present analysis, we restricted the dataset to the recent 30 years (1986–2015) and calculated the accumulated GDD required to reach BBCH 69 for each year and location using the simple average method and ERA5 mean daily air temperatures at 0.25° × 0.25° resolution (Hersbach et al. 2023; Copernicus Climate Change Service 2024), applying 4 °C as the lower temperature threshold (Zavalloni et al. 2006). This resulted in 37,980 GDD_4 estimates, which were used to fit a probability distribution representing the GDD requirement for sour cherry to reach the petal fall stage. This was done by first trimming the GDD_4 values to the 2nd–98th percentiles to exclude suspiciously low and high values due to potential observational errors and extreme microclimate effects and then fitting a lognormal distribution to the trimmed dataset (Figure 1b).

Date of tentative oviposition

Reissig et al. (1998) quantified the cumulative oviposition and feeding injury on apples over three years as a logistic function of accumulated GDD after petal fall using a temperature threshold of 10 °C and reported GDD_{10} values corresponding to the 40th and 60th percentiles of cumulative injury. We extracted additional percentile points from the published curve (Figure 1B in Reissig et al. 1998) using WebPlotDigitizer (https://automeris.io/) at approximately 10% intervals between 10% and 90% cumulative injury. This data was used to fit a probability distribution of GDD_{10} needed for oviposition after the petal fall, D_{ovi}, using a two-parameter logistic distribution (Figure 1c), with parameters estimated by fitting a linear regression. The distribution is used in the model to simulate the oviposition-ready date O_{tr}.

Simulating the realized oviposition date

Piñero and Prokopy (2006) showed that temperature accumulation is a stronger predictor of the spring immigration than host phenology, and therefore immigration date I_t and the petal fall date P_t are simulated as independent processes in our model:

$$I_t = inf\{t : GDD_{6.1}(t) \geq D_{imm}\}$$

$$P_t = inf\{t : GDD_4(t) \geq D_{pf}\}$$

Reissig et al. (1998) quantified the cumulative oviposition and feeding injury onwards from the petal fall. Consequently, in our model the oviposition-ready date O_{tr} is simulated as a function of GDD_{10} accumulated after the date of the petal fall P_t:

$$O_{tr} = inf\{t \geq P_t : GDD_{10}(t; P_t) \geq D_{ovi}\}$$

Piñero and Prokopy (2006) showed that immigration continues for one to three weeks after petal fall, suggesting that the early portion of the cumulative oviposition curve by Reissig et al. (1998) can partly reflect incomplete immigration of the pest at petal fall. To account for this, the realized oviposition date O_t is simulated in our model as follows:

$$O_t = max\{I_t, O_{tr}\}$$

Consequently, both the spring immigration and the oviposition after petal fall are simulated as independent processes in the model and the later of the two determines the realized oviposition date O_t. Since the cumulative oviposition curve by Reissig et al. (1998) was quantified from the petal fall of apple, it could under-, or overestimate realized oviposition on host species with substantially earlier or later petal fall. The current approach ensures that realized oviposition O_t is not underestimated by ensuring that oviposition cannot occur before the female has both immigrated and met the thermal requirements of oviposition.

Step 2: From oviposition to emergence of mature larvae from the fruits

The eggs of *C. nenuphar* are laid under the skin of the developing host fruit (Quaintance and Jenne 1912; Whitcomb 1929). After hatching the larvae tunnel deeper into the fruit to feed and subsequently develop through four instars (Whitcomb 1929; Chapman 1938). The larval development is strongly temperature-dependent (Whitcomb 1932) and influenced by the host plant species (Selby and Whalon 2014).

Lan et al. (2004) monitored the temperature-dependent development of the larvae of the southern strain of *C. nenuphar* and recorded the accumulated GDD needed for the larval development on apple using 11.1 °C as the lower and 35 °C as the upper development threshold. Later Selby and Whalon (2014) measured the accumulated $GDD_{11.1}$ needed for the egg hatching and larval development of the northern strain of *C. nenuphar* from different host plants using the parameters of Lan et al. (2004) in the calculations.

We used the outdoor sour cherry datasets (TNRC and CRC) reported by Selby and Whalon (2014) to fit a probability distribution of the accumulated $GDD_{11.1}$ required for egg hatching and larval development of the northern strain of *C. nenuphar* on sour cherry fruits, D_{lar}. Both datasets provide the mean and standard

deviation (SD) of accumulated $GDD_{11.1}$ for the larvae that emerged prior to fruit dissection, as well as the number of larvae still present in the fruits at the time of dissection. We first pooled the means and SDs of these datasets using fruit counts as weights and fitted a single normal distribution describing the accumulated $GDD_{11.1}$ required for egg hatching and larval development among the larvae that emerged from fruits. To incorporate the fraction of larvae that did not emerge, we constructed a large synthetic population in which the non-emerged larvae were assigned a $GDD_{11.1}$ value equal to the maximum value in the simulated sample of larvae that emerged from the fruits. We then fitted a normal distribution to this full synthetic dataset. This yielded a single probability distribution D_{lar} that reflects both the timing from egg hatching to larval emergence from fruits and the fraction of larvae that did not emerge from fruits during the experiments (Figure 1d). The distribution is used in the model to simulate the emergence of the mature larvae from fruits L_t of individual insects:

$$L_t = inf\{t \geq O_t : GDD_{11.1}(t; O_t) \geq D_{lar}\}$$

Step 3: From emergence of mature larvae from fruits to emergence of adults from the soil

After emerging from the fruit, mature larvae enter the soil to pupate (Crandall 1905; Quaintance and Jenne 1912; Whitcomb 1929; Chapman 1938). Prior to pupation, larvae may spend several days in the soil hollowing a pupal chamber (Lampasona et al. 2020). The duration of the pupal stage is strongly temperature-dependent (Whitcomb 1932; Lan et al. 2004; Selby and Whalon 2014) but is also influenced by soil moisture (Whitcomb 1929; Armstrong 1958; Chen and Scherm 2007).

Lan et al. (2004) monitored the temperature-dependent development of the pupal stage of the southern strain of *C. nenuphar* and recorded the accumulated GDD needed for the adults to emerge from soil using 8.7 °C as the development threshold temperature. Selby and Whalon (2014) subsequently measured the accumulated $GDD_{8.7}$ needed for the pupal development of the northern strain of *C. nenuphar*.

We used the results of Selby and Whalon (2014) to fit a probability distribution of accumulated $GDD_{8.7}$ needed for pupal development and emergence of adults of the northern strain of *C. nenuphar* D_{pupa}. This was done by pooling the mean accumulated $GDD_{8.7}$ and SD of the development times of pupae from four different indoor experiments reported in the study weighted by the number of pupation jars per host to obtain a single normal distribution for accumulated $GDD_{8.7}$ needed for the pupal development (Figure 1e). The distribution is used in the model to simulate the emergence of the new generation adults A_t of individual insects:

$$A_t = inf\{t \geq L_t : GDD_{8.7}(t; L_t) \geq D_{pupa}\}$$

Step 4: From emergence of adults from soil to overwintering

The adults of the northern strain of *C. nenuphar* undergo obligate diapause during the winter without completing the oogenesis in the autumn (Smith and Salkeld 1964). However, adults that emerge in late summer or autumn must still feed to accumulate sufficient energy reserves for overwintering (Quaintance and Jenne 1912; Smith and Salkeld 1964; Racette et al. 1992). After emergence, adults may feed for several weeks before entering diapause (Crandall 1905), but the exact duration and temperature requirements needed to build these overwintering reserves have not been quantified. It is also unknown whether adults emerging very late in autumn have adequate time to harden and successfully prepare for diapause.

Because detailed quantitative information on the duration of this period is lacking for *C. nenuphar*, we used the information available for *Anthonomus grandis* Boheman, 1843, another species in the family Curculionidae, which exhibits a similar life-history pattern, involving adult emergence followed by a feeding period prior to overwintering (Pereira et al. 2023). Studies on *A. grandis* indicate that diapause development occurs over a period of approximately 3 to 21 days following adult emergence under suitable environmental conditions, with most individuals transitioning within an intermediate time window during this period (Spurgeon and Raulston 2006; Spurgeon et al. 2018). Adult *C. nenuphar* are known to be active and feed at air temperatures ≥13 °C (Quaintance and Jenne 1912; Whitcomb 1932; Leskey and Zhang 2007). Accordingly, in the model the accumulation of overwintering reserves required for successful overwintering D_{fall} was defined as a probability distribution of the number of days with mean temperature ≥13 °C (Figure 1f). In the model, the distribution is used to simulate the completion of the life cycle and the onset of overwintering readiness F_t for individual insects:

$$F_t = inf\left\{t \geq A_t : \sum_{u=A_t}^{t} I(T_u \geq 13℃) \geq D_{fall}\right\}$$

where T_u is the daily mean temperature on day u, and $I(\cdot)$ is an indicator function equal to 1 when the condition is met and 0 otherwise.

Given the uncertainty associated with transferring species-specific traits from *A. grandis* to *C. nenuphar*, we applied a scenario based approach to evaluate the sensitivity of model outcomes to assumptions regarding the overwinter readiness. Consequently, three alternative probability distributions for D_{fall} were defined as truncated normal distributions, representing different portions of the observed diapause development range

for *A. grandis* but extending the lower and upper bounds slightly to account for uncertainty at the extremes (Figure 1f).

The "fast" scenario (mean = 5 days, SD = 2.5 days; truncated to 2–9 days) represents a situation in which the adults become ready for overwintering soon after emergence from the soil. The "intermediate" scenario (mean = 9 days, SD = 3 days; truncated to 5–14 days) reflects the central tendency of the proxy data and corresponds to the period during which diapause incidence increases most rapidly for *A. grandis*. The "slow" scenario (mean = 14 days, SD = 4 days; truncated to 9–25 days) represents delayed overwintering readiness. The SD for each scenario was selected so that approximately 80–90% of the probability mass of the underlying normal distributions falls within the specified truncation bounds.

Although the true quantitative requirements for overwintering readiness in *C. nenuphar* remain unknown, the selected scenarios are expected to encompass most biologically plausible variation in this process. It is unlikely that overwintering readiness would generally require fewer suitable feeding days than assumed in the "fast" scenario or substantially more than assumed in the "slow" scenario, even though the most likely response may lie within or between the scenarios. Thus, the scenario approach provides a broad representation of uncertainty in the accumulation of overwintering reserves required for successful overwintering.

Growing degree days calculations

The model requires mean daily air-temperature data for the entire calendar year (in °C) to calculate GDD and to determine the dates on which the assumed GDD requirements for the developmental steps are met. The GDD values for steps 1 (date of oviposition) and 3 (date of adult emergence after pupation) are calculated using the simple average method.

Step 2 (date of larval emergence from fruit) is calculated using the GDD model originally described by Lan et al. (2004) and later used by Selby and Whalon (2014). This model uses both a lower and upper developmental threshold (11.1°C and 35°C, respectively) and applies correction factors for temperatures above 30°C.

However, Selby and Whalon (2014) noted that the original GDD model by Lan et al. (2004) predicts zero development between 33 and 35 °C, which contradicts the empirical development reported at these temperatures. To address this, they introduced a short linear function ($26.85 - 0.45T$) to provide at least some GDD accumulation within this range (see Figure 1 in Selby and Whalon, 2014).

When implementing this correction, we found that an additional small adjustment was necessary to ensure that the resulting GDD values precisely match the curve shown in Figure 1 by Selby and Whalon (2014). Specifically, the corrected function for the range 33–35 still needs to have the lower developmental threshold (11.1 °C) subtracted, which is not stated explicitly by Selby and Whalon (2014). Applying this adjustment allows the model to reproduce the intended decline from approximately 1 GDD at 33 °C to 0 GDD at 35 °C.

Accordingly, the GDD contribution for a day with mean temperature T is calculated as follows:

$$GDD(T) = \begin{cases} 0, & T \leq 11.1 \\ T - 11.1, & 11.1 < T \leq 30 \\ 210 - 6T - 11.1 & 30 < T \leq 33 \\ 26.85 - 0.45T - 11.1, & 33 < T < 35 \\ 0, & T \geq 35 \end{cases}$$

Evaluating the model performance

Before applying the model to assess the northern limit of the potential range of the northern strain of *C. nenuphar* in Europe, we first evaluated its performance within the native range of the pest. This was done by running the model across the cross-border region spanning the United States and Canada (North: 53°, West: -105°, South: 39°, East: -57°), where the northern limit of the natural distribution of *C. nenuphar* occurs (Chapman 1938). The historical range map of *C. nenuphar* by Chapman (1938) was georeferenced with a third-order polynomial transformation and manually assigned control points evenly distributed across the area using ArcGIS Pro (Esri, Redlands, CA, USA). To evaluate the sensitivity of predictions to uncertainty in the thermal requirement for overwintering readiness F_t, simulations were repeated under three alternative scenarios ("fast", "intermediate" and "slow").

The model was driven with ERA5 mean daily air temperatures at 0.25° × 0.25° resolution (Hersbach et al. 2023; Copernicus Climate Change Service 2024) for the years 1940–1959, which represents the closest 20-year period with available climate data corresponding to the most detailed available distribution map of *C. nenuphar* provided by Chapman (1938). Each simulation was run with 500 stochastic iterations.

Model performance was assessed using two complementary metrics. The first metric, the mean life cycle completion proportion, was calculated as the average proportion of iterations in which the full life cycle was completed across the 20-year period. This metric provides an overview of the general thermal suitability across the whole period. The second metric, proportion of successful years, was calculated as the proportion

of years in which at least one iteration indicated successful completion of the life cycle. This metric captures interannual temperature variability and indicates how often conditions meet the minimum requirements for development. While these metrics were essentially meant to evaluate model performance, they were also used to calibrate how simulated life cycle completion levels should be interpreted when the model was subsequently applied to Europe.

To evaluate model performance, outputs were summarized across four spatial zones defined by two distance bands (0–50 km and 50–200 km) and their position relative to the georeferenced historical range limit of *C. nenuphar* (inside vs. outside the range). The narrow 0–50 km band describes model behavior immediately adjacent to the historical range limit, whereas the 50–200 km band describes the behavior between areas clearly within and beyond the historical range. For each zone and scenario, we summarized both performance metrics, i.e. the mean life cycle completion proportion and the proportion of successful years. Sensitivity among the three scenarios for overwintering readiness F_t was quantified using the SD among the scenarios and the mean difference between the most and least permissive scenarios. In addition, cell-level SDs among the three scenarios were mapped to identify geographical areas where predictions were most sensitive to assumptions about F_t.

Assessing the potential northern range limit of *C. nenuphar* in Europe

To estimate the potential northern range limit of the northern strain of *C. nenuphar* in the current European climate, we ran the model for northern and central Europe (North: 71°, West: -15°, South: 47°, East: 45°) using ERA5 mean daily air temperatures at 0.25° × 0.25° resolution for the years 2006–2025 (Hersbach et al. 2023; Copernicus Climate Change Service 2024), using 500 stochastic iterations consistent with the native-range analysis. As in the native-range analysis, the estimation was based on the two metrics, the mean life cycle completion proportion and the proportion of successful years. To evaluate the sensitivity of predictions to uncertainty in the thermal requirement for overwintering readiness F_t, simulations were repeated under three alternative scenarios (“fast”, “intermediate” and “slow”). In addition, cell-level SDs among the three scenarios were mapped to identify geographical areas where predictions were most sensitive to assumptions about F_t.

To assess potential future range expansion of the northern strain of *C. nenuphar* in Europe, we estimated the northern limit of the potential range using climate projections for the period 2041–2060. Daily near-surface air temperature data for 2041–2060 were obtained from an eight-member CMIP6 multi-model ensemble under the SSP2-4.5 forcing scenario, which represents a “middle-of-the-road” socioeconomic pathway and an intermediate greenhouse-gas emission trajectory (Eyring et al. 2016; O’Neill et al. 2016; Meinshausen et al. 2020). Because these CMIP6 data were available as daily, year-specific time series, the simulations could account for interannual variability in temperature conditions during 2041–2060. The selected ensemble

consisted of eight CMIP6 models from different modelling centers with varying spatial resolution (Table 2) and they were chosen based on (i) the availability of daily temperature data from the Climate Data Store (CDS) of the Copernicus Climate Change Service (Copernicus Climate Change Service 2021) and (ii) their demonstrated ability to reproduce temperature patterns in northern Europe, as assessed using the GCMeval tool (Parding et al. 2020). In this evaluation framework, models were ranked according to their performance across seasonal temperature variables using equally weighted skill metrics. These metrics included absolute bias relative to reference data, spatial correlation, spatial standard deviation, and the root mean square error of the mean annual cycle (Parding et al. 2020). In addition to model performance and data availability, we ensured structural diversity within the ensemble by avoiding multiple models from the same climate modelling center. The stochastic phenology model was run independently for each CMIP6 model for each year from 2041 to 2060, with 500 stochastic iterations. For each CMIP6 model, we calculated the mean life cycle completion proportion and the proportion of successful years. For the future projections, the second metric was calculated across the 160 CMIP6 model-year combinations and is referred to as the proportion of successful model-years. It was defined as the proportion of model-year combinations in which at least one iteration indicated successful completion of the life cycle. Both metrics were calculated under the three alternative scenarios for F_t. Finally, the simulation outputs were resampled to a uniform grid defined by the finest resolution model in the ensemble (0.5° × 0.5°) and then summarized across the CMIP6 multi-model ensemble to project the future establishment potential under the SSP2-4.5 conditions for the mid-21st century.

Table 2. CMIP6 global climate models used for the mid-21st-century climate projections. Daily mean near-surface air temperature data were obtained from the Climate Data Store of the Copernicus Climate Change Service under SSP2-4.5 for each year from 2041 to 2060.

CMIP6 model	**Ensemble member**	**Institution description**
CMCC-ESM2	r1i1p1f1	Fondazione Centro Euro-Mediterraneo sui Cambiamenti Climatici, Lecce, Italy
CNRM-CM6-1	r1i1p1f2	CNRM–CERFACS, Toulouse, France
GFDL-ESM4	r1i1p1f1	National Oceanic and Atmospheric Administration, Geophysical Fluid Dynamics Laboratory, Princeton, NJ, USA
IPSL-CM6A-LR	r1i1p1f1	Institut Pierre Simon Laplace, Paris, France
MPI-ESM1-2-LR	r10i1p1f1	Max Planck Institute for Meteorology, Hamburg, Germany
MRI-ESM2-0	r1i1p1f1	Meteorological Research Institute, Tsukuba, Japan
NorESM2-LM	r1i1p1f1	NorESM Climate modeling Consortium, Norway
UKESM1-0-LL	r1i1p1f2	Met Office Hadley Centre, Exeter, UK

Results

The model performance in the native range of *C. nenuphar*

The model reproduced expected patterns in thermal suitability across the historical northern range limit of *C. nenuphar*. For both metrics, the mean life cycle completion proportion and the proportion of successful years, values were higher inside than outside the range limit (Table 3; Figure 2). The contrast was clearest in the 50–200 km zones. Within these zones, the mean life cycle completion proportion was high inside the range but much lower outside it, whereas the proportion of successful years was close to 1 inside the range and remained relatively high even outside it.

Sensitivity among the three scenarios for overwintering readiness F_t was generally moderate but varied between the metrics and spatial zones (Table 3; Figure 3). For the mean life cycle completion proportion, sensitivity was highest near the historical range limit and was relatively similar on both sides of the limit, with mean differences among scenarios of approximately 0.06–0.08. In contrast, sensitivity in the proportion of successful years was low inside the historical range but increased outside the range, where the mean difference among scenarios reached 0.169. This pattern indicates that conditions inside the range were generally suitable enough for at least some simulated individuals to complete the full life cycle in all years, regardless of the F_t scenario.

Overall, the modelling results suggest that thermal suitability declines gradually towards the northern range limit, but within the range conditions are still suitable for at least part of the population to complete the full life cycle in all years. This is also reasonable biologically as conditions may occasionally be suitable for completing the life cycle even beyond the range, but establishment requires that at least a part of the population completes the life cycle every year, although limited potential adult carry-over between years may buffer populations against occasional unfavorable seasons. Long-term temperature averages conceal interannual variability and fail to capture the consequences of exceptional years. For example, repeated unusually cool summers could prevent the completion of the life cycle and thereby hinder establishment, even if long-term averages suggest overall climatic suitability.

Table 3. Model outputs and sensitivity summaries among the “fast”, “intermediate” and “slow” F_t scenarios within the spatial zones inside and outside the georeferenced historical northern range limit of *C. nenuphar*. Values are shown for the mean life cycle completion proportion across 1940–1959 and for the proportion of successful years. SD is the mean standard deviation among the three F_t scenarios, and DIFF is the mean difference between the most and least permissive scenarios.

Metric	Zone	Fast	Intermediate	Slow	SD	DIFF

The mean life cycle completion proportion	Inside 0–50 km	0.69	0.66	0.61	0.042	0.083
	Inside 50–200 km	0.84	0.81	0.77	0.035	0.07
	Outside 0–50 km	0.51	0.47	0.43	0.04	0.08
	Outside 50–200 km	0.28	0.25	0.22	0.029	0.059
The proportion of successful years	Inside 0–50 km	0.95	0.93	0.9	0.027	0.051
	Inside 50–200 km	0.99	0.98	0.97	0.01	0.018
	Outside 0–50 km	0.87	0.82	0.77	0.053	0.103
	Outside 50–200 km	0.7	0.6	0.53	0.088	0.169

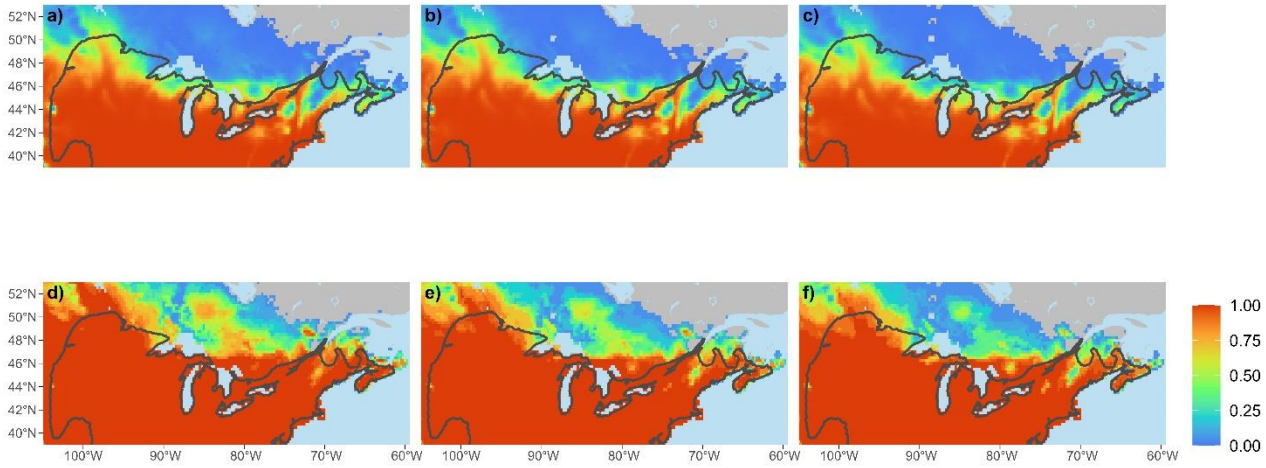


Figure 2. Maps a–c show the mean life cycle completion proportion across 1940–1959 under the "fast", "intermediate" and "slow" F_t scenarios, respectively. Maps d–f show the proportion of successful years under the same scenarios. The grey line indicates the georeferenced historical range limit of *C. nenuphar* from Chapman (1938).

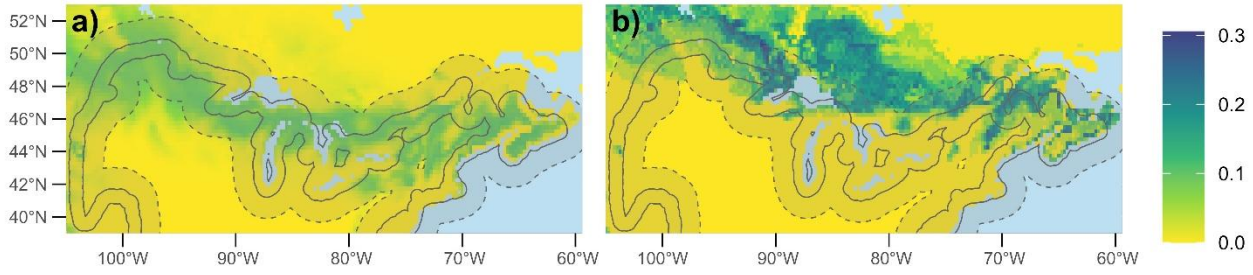


Figure 3. Standard deviation among the "fast", "intermediate" and "slow" F_t scenarios for (a) the mean life cycle completion proportion across 1940–1959 and (b) the proportion of successful years. Solid lines indicate the 0–50 km

band and dashed lines the 50–200 km band around the georeferenced historical range limit of *C. nenuphar* from Chapman (1938).

The northern range limit in Europe

Current climate (2006–2025)

Under the modelling assumptions and the 2006–2025 climate, both metrics, the mean life cycle completion proportion and the proportion of successful years, were close to 1 across much of central Europe and declined northwards through the United Kingdom, northern Germany and Poland, approaching zero in northern Finland and Sweden, most of Norway, and Scotland (Figure 4). Central Europe therefore appears thermally suitable for the northern strain of *C. nenuphar*, whereas Finland, Scotland, and most of Estonia, Ireland, Norway and Sweden appear unsuitable. In these unsuitable areas, a large proportion of individuals failed to complete the life cycle across the 20-year period and, in several years, no individuals reached overwintering readiness regardless of the F_t scenario (Figure 4). Establishment under these conditions therefore appears unlikely.

Between these extremes lies a transition region, including the southern and central United Kingdom, northern Germany and Poland, Denmark, the Baltic states and southernmost Scandinavia, where the thermal suitability declined gradually. Across the whole study area, the F_t scenario had little effect on the overall geographical pattern of thermal suitability. However, within the transition region it clearly influenced the mean life cycle completion proportion, and in the northern part of the transition region and especially in the adjacent less suitable areas it also influenced the proportion of successful years (Figure 5).

The southern parts of the transition region, including the southern United Kingdom, northern Germany and Poland, and most of Lithuania, still appeared thermally suitable for establishment of *C. nenuphar*, with a mean life cycle completion proportion above 0.5 and a proportion of successful years equal to 1 regardless of the F_t scenario (Figure 4). In much of the remaining transition region, however, the mean life cycle completion proportion was close to or below 0.5, depending on the F_t scenario. Nevertheless, in the central United Kingdom, northern Denmark, Latvia, and localized coastal cells in western Estonia, southern Ireland and southernmost Scandinavia, at least one life cycle completion was achieved in every year under the more permissive F_t scenarios. Because these outcomes depend strongly on the assumed F_t values, establishment across this part of the transition region cannot be confidently classified as either likely or unlikely.

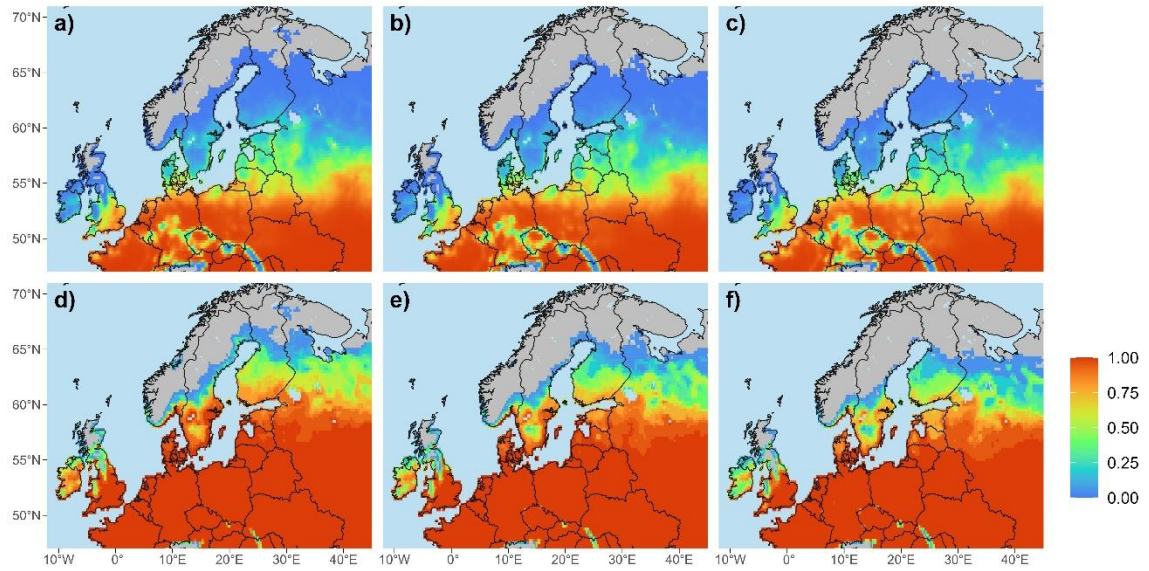


Figure 4. Maps a–c show the mean life cycle completion proportion across 2006–2025 under the "fast", "intermediate" and "slow" F_t scenarios, respectively. Maps d–f show the proportion of successful years under the same F_t scenarios.

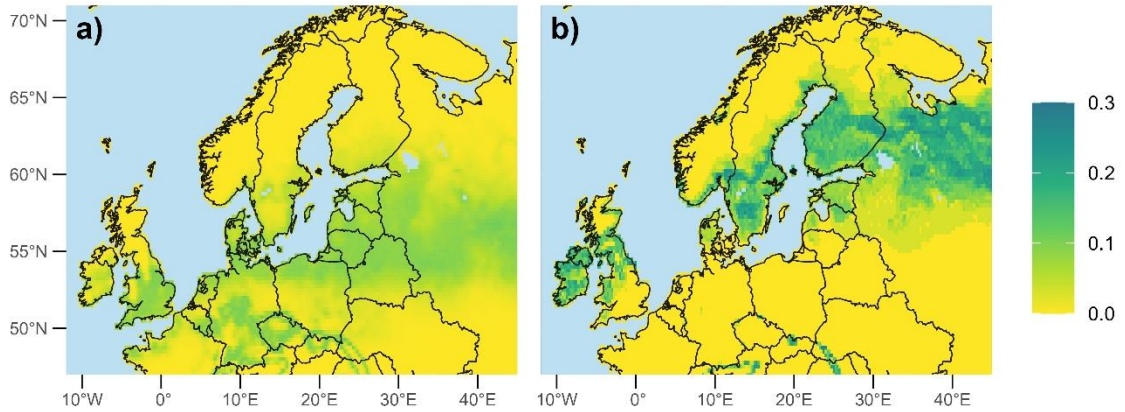


Figure 5. Standard deviation among the "fast", "intermediate" and "slow" F_t scenarios for (a) the mean life cycle completion proportion across 2006–2025 and (b) the proportion of successful years.

Future climate (2041–2060)

Under the 2041–2060 CMIP6 multi-model ensemble projections for SSP2-4.5, the geographical pattern of thermal suitability remained broadly similar to that under the current climate, with high suitability across central Europe and declining suitability towards the north (Figure 6). However, the transition region shifted northwards, extending into the northern United Kingdom and Ireland, the Baltic region, Denmark, and southern Sweden and Finland. As under the current climate, the F_t scenario influenced the simulated life cycle completion proportions within and north of the transition region but had little effect on the overall geographical pattern (Figure 7).

Several areas where the potential establishment of *C. nenuphar* was uncertain under the current climate became more suitable under the future projections. In Estonia, southern Ireland and southern Sweden, roughly half or more of the simulated individuals reached overwintering readiness, depending on the F_t scenario. Successful life cycle completion was also achieved in all or nearly all CMIP6 model-years, indicating that at least part of a population could complete the annual life cycle across most projected model-year combinations.

Thermal suitability also increased in southern and central Finland. However, a large proportion of individuals still failed to complete the life cycle, and in several CMIP6 model-years no individuals reached overwintering readiness under any F_t scenario. Establishment of *C. nenuphar* therefore appears to remain unlikely across Finland even in the mid-21st-century SSP2-4.5 projections.

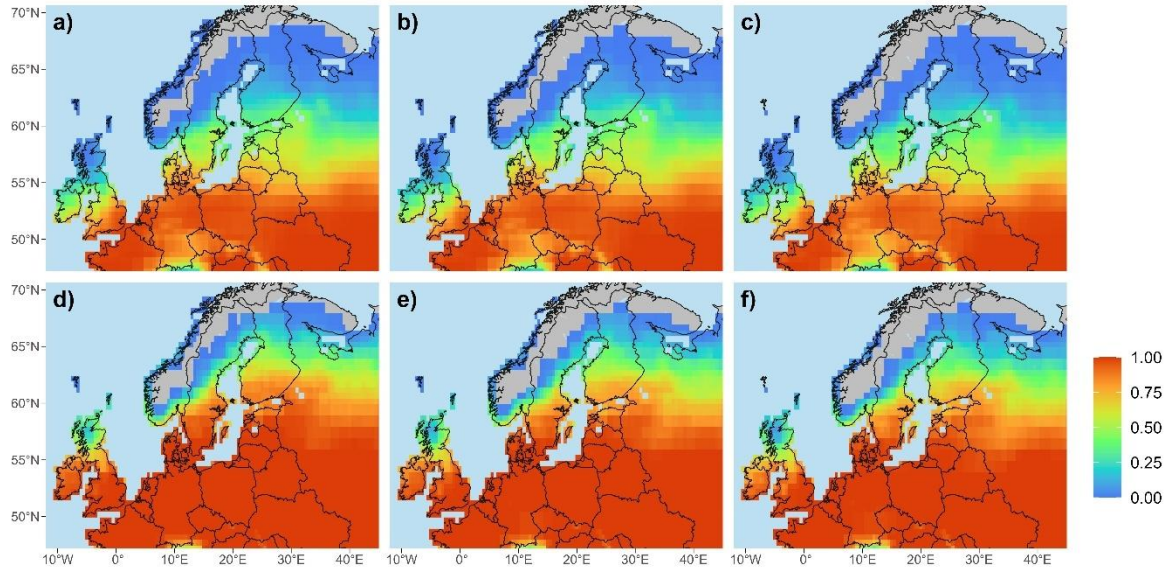


Figure 6. The projected life cycle completion by the northern strain of *C. nenuphar* in Europe for 2041–2060 based on the CMIP6 multi-model ensemble under SSP2-4.5. Maps a–c show the mean life cycle completion proportion under the "fast", "intermediate" and "slow" F_t scenarios, respectively. Maps d–f show the proportion of successful model-years under the same F_t scenarios.

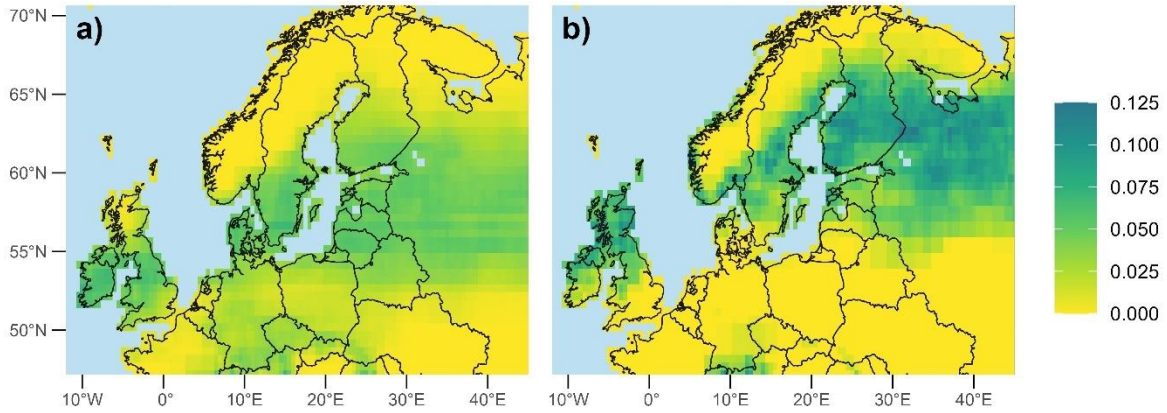


Figure 7. Standard deviation among the "fast", "intermediate" and "slow" F_t scenarios for (a) the mean life cycle completion proportion across 2041–2060 based on the CMIP6 multi-model ensemble under SSP2-4.5 and (b) the proportion of successful model-years.

Discussion

Implications for risk management

EU plant health legislation identifies 20 priority pests, including *C. nenuphar*, as Union quarantine pests with potentially severe economic, environmental, or social impacts (European Parliament and Council of the European Union 2016; European Commission 2019). Member States are therefore required to conduct extensive surveillance and implement measures to prevent the introduction and spread of these pests within their territories. However, the EU encompasses a wide diversity of cropping systems, forest types, and ecoclimatic conditions, and consequently not all priority pests are necessarily able to establish and spread across all Member States, particularly where host plants are absent or climatic conditions are unsuitable.

EU legislation recognizes this variability and allows that, where it can be unequivocally demonstrated that a priority pest is unable to establish or spread due to unsuitable ecoclimatic conditions or lack of hosts, the implementation of certain official measures is not necessary (European Parliament and Council of the European Union 2016). To this end, several recent studies have evaluated the establishment potential of priority pests in northern EU Member States, where cooler climatic conditions may constrain pest development and survival (Björklund and Boberg 2020a; 2020b; Boberg and Björklund 2020a; 2020b; 2020c; Tuomola et al. 2021; Tuomola and Hannunen 2024; Tuomola 2025). The present study contributes to this body of work by providing a detailed assessment of the establishment potential of *C. nenuphar* under current and future climatic conditions in northern Europe.

Our modelling results indicate that, within the EU, current temperature conditions in Finland, most of Ireland and Sweden, and parts of the Baltic region are thermally unsuitable for the northern strain of *C. nenuphar* on sour cherry. In these areas, the mean life cycle completion proportion was generally low across the 20-year period, and multiple years passed without any successful completion, suggesting that the likelihood of establishment is very low. Under the 2041–2060 CMIP6 multi-model ensemble projections for SSP2-4.5, thermal suitability increased in these areas but remained below levels indicating likely establishment in the northernmost parts of the EU. For example, establishment of *C. nenuphar* appears unlikely across Finland even in the 2041–2060 projections under SSP2-4.5.

Taken together, our results provide modelling-based information on the establishment potential of *C. nenuphar* under current and projected future climatic conditions that can support risk managers in northern EU Member States in evaluating where official surveillance for *C. nenuphar* is warranted. Nevertheless, the use of these results in official risk management should be considered in the context of previous studies and considering the uncertainties and limitations outlined in the following sections.

Comparison with previous studies

Our modelling results are broadly consistent with those of Boberg and Björklund (2020b), who concluded, based on GDD accumulation under current climate, that summer temperatures in Sweden allow completion of the life cycle of *C. nenuphar* within a single season only in the southern part of the country. The present study extends the analysis by Boberg and Björklund (2020b) by applying a more comprehensive phenological modelling framework that incorporates intraspecific variation within the northern strain of *C. nenuphar* and covers a broader geographic region across central and northern Europe.

In contrast, our results do not support the conclusions of EFSA (2018a, 2019, 2025), which suggest that climatic conditions are unlikely to limit the establishment of *C. nenuphar* in Europe. In the pest categorization of *C. nenuphar* (EFSA 2018a), this conclusion is primarily based on the occurrence of Köppen–Geiger climate types within the native range of the pest and the presence of similar climate types within the EU. In the context of pest risk assessment, the Köppen–Geiger classification is generally regarded as a preliminary screening tool that provides a coarse estimate of climatic suitability (Kriticos et al. 2024; EFSA 2026). In other words, it does not account for finer-scale climatic variation within the climate types and therefore cannot capture the detailed constraints that determine whether local conditions are suitable for species establishment. The phenological modelling approach applied in the present study extends the EFSA (2018a) assessment by showing that not all areas within the Köppen–Geiger climate types where the pest occurs in its native range and which are also present in Europe are necessarily suitable for establishment. Comparison with EFSA's pest reports supporting the ranking of candidate priority pests (EFSA 2019, 2025) is more challenging, as the methodological basis underlying these conclusions is not fully documented.

To our knowledge, our study represents the first attempt to assess the establishment potential of *C. nenuphar* under future climatic conditions. While the use of multiple climate scenarios is generally recommended in pest risk assessment (Rosace et al. 2024), we based our projections on a single scenario, SSP2–4.5, which combines the "middle-of-the-road" SSP2 socioeconomic storyline with an intermediate radiative forcing level of 4.5 W/m^2 by 2100 (O'Neill et al. 2016; Meinshausen et al. 2020). Inclusion of additional scenarios would strengthen the robustness and usability of the assessment. However, this was not possible, as daily climate data for the same time period and for the same GCM realizations were not available for the other SSP scenarios.

Limitations and sources of uncertainty

Despite the strong empirical basis of the modelling framework, several limitations and uncertainties should be acknowledged.

First, the model integrates results from individual studies, each focusing on specific life stages of *C. nenuphar* (Reissig et al. 1998; Piñero and Prokopy 2006; Selby and Whalon 2014). Although all studies concern the northern strain, they were conducted on different populations and under varying environmental conditions. If *C. nenuphar* exhibited strong local adaptation, combining data from populations adapted to different environmental conditions could introduce bias and reduce the accuracy of the model. However, we found no evidence from previous studies of pronounced adaptive differentiation in *C. nenuphar* (e.g. Racette et al. 1992; Zhang et al. 2008; Lampasona et al. 2020), suggesting that the integration of these data does not substantially compromise model validity. Nevertheless, the framework could be further strengthened by incorporating multiple independent studies for each life stage, which would better capture potential variation in population responses across the geographic range of the northern strain.

A key uncertainty relates to the modelling of overwintering readiness (step 4), for which no *C. nenuphar* specific quantitative empirical data are currently available. This modelling step was therefore parameterized using proxy information from *A. grandis*, a species with a comparable life-history strategy involving post-emergence feeding prior to overwintering (Pereira et al. 2023). Sensitivity analyses using alternative scenario assumptions for overwintering readiness F_t showed that model outcomes in transition regions, where the thermal suitability gradually declines from suitable to unsuitable, are particularly influenced by the selected scenario. While defining a precise northern range limit for *C. nenuphar* in northern Europe would be inherently difficult even under ideal data conditions, the additional uncertainty associated with the overwintering readiness further increases the overall uncertainty of the thermal suitability in these transition regions.

Another uncertainty concerns the representation of oviposition timing (step 1). In the northern strain of *C. nenuphar*, females undergo an obligatory winter diapause without completing oogenesis (Smith and Salkeld 1964). Consequently, before oviposition in the spring the females need to complete the oogenesis. The timing of oocyte maturation is independent of mating (Hoffmann et al. 2004) and when the mating occurs before oocyte maturation, the female stores the sperm in spermatheca and continues oocyte development until the oocytes reach the maturity for oviposition (Leskey 2008). While our model does not explicitly simulate these physiological processes, empirical evidence indicates that most females are mated before the fruit set stage (BBCH 71) (Hoffmann et al. 2004). Thus, spring emergence and movement to host trees D_{imm} and oviposition after the petal fall D_{ovi} were considered reasonable proxies of the realized oviposition timing O_t. While this simplification seems biologically justified, it does not explicitly capture all underlying physiological processes of the species.

A further uncertainty concerns demographic carry-over between years through extended adult longevity, which is not represented in our framework because establishment is assessed based on completion of the life cycle within a single season. Armstrong (1958) found that some adults survived into the following season under optimum insectary conditions, but that longevity under field conditions was considerably lower. There is therefore no clear evidence that carry-over acts as an effective persistence mechanism in the field, and it is least likely to do so in climatically marginal areas, whose conditions are furthest from those under which prolonged survival was observed. We therefore interpret extended adult longevity as a possible buffer against occasional unfavorable years in otherwise suitable areas, rather than as a mechanism that could sustain populations where thermal conditions consistently preclude life cycle completion. Nevertheless, because such carry-over is physiologically possible and is not captured by the model, it remains a genuine source of uncertainty, and our requirement for life cycle completion in nearly every year may be somewhat conservative for climatically marginal areas if carry-over occurs in the field.

Our model is driven solely by daily air temperatures, whereas other environmental factors may also influence development and establishment of *C. nenuphar*. For example, soil moisture can affect the duration of the pupal stage (Whitcomb 1929; Armstrong 1958; Chen and Scherm 2007), and photoperiod influences adult activity and diapause regulation (McGiffen et al. 1987). Incorporating these factors would improve model realism, but due to lack of data on how these factors contribute to the development of *C. nenuphar*, they could not be included in the modelling framework.

The applicability of the model is limited to the northern strain of *C. nenuphar* and to sour cherry as the host plant. While the overall model structure could be applied to the southern strain as well, differences in the temperature-dependent development between the northern and southern strains (Hoffmann et al. 2004; Lan et al. 2004; Selby and Whalon 2014) require that the underlying parameterization should be based on empirical

data specific to the southern strain. Similarly, host-specific differences in phenology and larval development rates limit direct extrapolation of the model to other host species (Selby and Whalon 2014).

Finally, we ran the simulations with 500 iterations, which represents a practical balance between computational cost and adequate sampling of stochastic variability. Increasing the number of iterations further, e.g. to several thousand, becomes impractical within the framework that integrates daily climate data over multiple years and across large geographical areas. Although 500 iterations do not provide fully stable distributions and do not necessarily fully capture the most extreme outcomes, they provide sufficient coverage of the possible trajectories to reliably assess establishment potential. Moreover, this level of iterations is appropriate for representing a potential founder population in Europe, which is likely to consist of relatively few individuals.

Conclusion

Since the number of potentially harmful non-indigenous plant pests is large, it is essential that the limited resources available for official plant health surveillance aimed at preventing the introduction and spread of these pests are directed towards those posing the greatest risk. *Conotrachelus nenuphar* is considered a significant potential threat to plant health in the EU and is therefore classified as a priority pest under EU plant health legislation. Under this legislation, all EU Member States are required to implement strict surveillance measures for each priority pest aimed at preventing their introduction and facilitating early detection of possible outbreaks. However, if it can be clearly demonstrated that a priority pest is unable to establish or spread because of unsuitable ecoclimatic conditions or the absence of suitable hosts, certain official measures may be considered unnecessary. Our stochastic phenology model, which simulates the temperature-dependent development of the northern strain of *C. nenuphar* on sour cherry and evaluates whether its life cycle can be completed within a single calendar year under given climatic conditions, indicates that not all regions of northern Europe are thermally suitable for its establishment. This applies both to the current climate and to mid-21st-century climate projections under the SSP2-4.5 scenario. These modelling results can support EU risk managers in evaluating where official surveillance for *C. nenuphar* is justified and where resources could potentially be allocated more efficiently. Given the wide diversity of cropping systems, forest types, and ecoclimatic conditions across the EU, similar studies on the establishment potential of other pests regulated under EU plant health legislation are needed to support the efficient allocation of official plant health resources throughout the Union.

References

Armstrong T (1958) Life-history and ecology of the plum curculio, *Conotrachelus nenuphar* (Hbst.) (Coleoptera: Curculionidae), in the Niagara Peninsula, Ontario. Can Entomol 90:8–17. https://doi.org/10.4039/Ent908-1

Baker RHA (2002) Predicting the limits to the potential distribution of alien crop pests. In: Hallman GJ, Schwalbe CP (eds) Invasive arthropods in agriculture: problems and solutions. Science Publishers, Enfield, pp 207–241

Björklund N, Boberg J (2020a) Potential establishment of the priority pest *Anthonomus eugenii* in Sweden. Swedish University of Agricultural Sciences. https://research.slu.se/files/19209433/fulltext.pdf

Björklund N, Boberg J (2020b) Potential establishment of the priority pest *Popillia japonica* in Sweden. Swedish University of Agricultural Sciences. https://research.slu.se/files/19234683/fulltext.pdf

Boberg J, Björklund N (2020a) Potential establishment of the priority pest *Bactericera cockerelli* in Sweden. Swedish University of Agricultural Sciences. https://research.slu.se/files/19152270/fulltext.pdf

Boberg J, Björklund N (2020b) Potential establishment of the priority pest *Conotrachelus nenuphar* in Sweden. Swedish University of Agricultural Sciences. https://research.slu.se/ws/portalfiles/portal/19124851/fulltext.pdf

Boberg J, Björklund N (2020c) Potential establishment of the priority pest *Rhagoletis pomonella* in Sweden. Swedish University of Agricultural Sciences. https://research.slu.se/ws/portalfiles/portal/19259263/fulltext.pdf

Burne AR (2019) Pest risk assessment: *Halyomorpha halys*, brown marmorated stink bug. Version 1, June 2019. Ministry for Primary Industries, New Zealand

Chapman PJ (1938) The plum curculio as an apple pest. Bulletin of the New York State Agricultural Experiment Station 684:1–75

Chaves B, Salazar MR, Schmidt T, Dasgupta N, Hoogenboom G (2017) Modeling apple bloom phenology. Acta Hortic 1160:201–206. https://doi.org/10.17660/ActaHortic.2017.1160.29

Chen H, Scherm H (2007) Moisture effects on development and survival of the plum curculio (Coleoptera: Curculionidae). J Entomol Sci 42:207–216. https://doi.org/10.18474/0749-8004-42.2.207

Copernicus Climate Change Service, Climate Data Store (2021) CMIP6 climate projections. Copernicus Climate Change Service (C3S) Climate Data Store (CDS). https://doi.org/10.24381/cds.c866074c

Copernicus Climate Change Service, Climate Data Store (2024) ERA5 post-processed daily-statistics on single levels from 1940 to present. Copernicus Climate Change Service (C3S) Climate Data Store (CDS). https://doi.org/10.24381/cds.4991cf48

Crandall CS (1905) The curculio and the apple. Illinois Agricultural Experiment Station Bulletin 98:467–560

EFSA (European Food Safety Authority), Baker R, Gilioli G, Behring C, Candiani D, Gogin A, Kaluski T, Kinkar M, Mosbach Schulz O, Neri FM, Preti S, Rosace MC, Siligato R, Stancanelli G, Tramontini S (2019) Conotrachelus nenuphar – Pest report and datasheet to support ranking of EU candidate priority pests. Zenodo. https://doi.org/10.5281/zenodo.2789434

EFSA (European Food Safety Authority), Tramontini S, Baldassarre F, Binazzi F, Gilioli G, Mastin A, Rzpecka D, Scala M, Sánchez B, Nougadère A, Vos S (2025) *Conotrachelus nenuphar* – Pest report to support the ranking of EU candidate priority pests. EFSA Supporting Publication 2025:EN-9442. https://doi.org/10.2903/sp.efsa.2025.EN-9442

EFSA PLH Panel (EFSA Panel on Plant Health), Jeger M, Bragard C, Caffier D, Candresse T, Chatzivassiliou E, Dehnen Schmutz K, Gilioli G, Gregoire JC, Jaques Miret JA, MacLeod A, Niere B, Parnell S, Potting R, Rafoss T, Rossi V, Urek G, Van Bruggen A, Van der Werf W, West J, Winter S, Bergeretti F, Björklund N, Mosbach Schulz O, Vos S, Navajas Navarro M (2017) Scientific opinion on the pest risk assessment of *Eotetranychus lewisi* for the EU territory. EFSA J 15:4878. https://doi.org/10.2903/j.efsa.2017.4878

EFSA PLH Panel (EFSA Plant Health Panel), Bragard C, Dehnen Schmutz K, Di Serio F, Gonthier P, Jacques MA, Jaques Miret JA, Justesen AF, Magnusson CS, Milonas P, Navas Cortes JA, Parnell S, Potting R, Reignault PL, Thulke HH, Van der Werf W, Vicent Civera A, Yuen J, Zappalà L, Czwienczek E, MacLeod A (2018a) Pest categorisation of *Conotrachelus nenuphar*. EFSA J 16:5437. https://doi.org/10.2903/j.efsa.2018.5437

EFSA (European Food Safety Authority), Rossi E, Maiorano A, Gobbi A (2026) Update of the Köppen–Geiger climate classification for EFSA PLH risk assessment. EFSA J 24:e9859. https://doi.org/10.2903/j.efsa.2026.9859

EFSA PLH Panel (EFSA Plant Health Panel), Bragard C, Dehnen Schmutz K, Di Serio F, Gonthier P, Jacques MA, Jaques Miret JA, Justesen AF, Magnusson CS, Milonas P, Navas Cortes JA, Parnell S, Potting R, Reignault PL, Thulke HH, Van der Werf W, Vicent Civera A, Yuen J, Zappalà L, Czwienczek E, MacLeod A (2018b) Pest categorisation of *Popillia japonica*. EFSA J 16:5438. https://doi.org/10.2903/j.efsa.2018.5438

EPPO (2024) Pest risk analysis for *Chloridea virescens*. EPPO Technical Document No. 1091. EPPO, Paris. https://gd.eppo.int/taxon/HELIVI/documents

European Commission (2019) Commission Delegated Regulation (EU) 2019/1702 establishing the list of priority pests. Off J Eur Union L 260:8–10. https://data.europa.eu/eli/reg_del/2019/1702/oj

European Parliament and Council of the European Union (2016) Regulation (EU) 2016/2031 on protective measures against pests of plants. https://data.europa.eu/eli/reg/2016/2031

Eyre D, Baker RHA, Brunel S, Dupin M, Jarošík V, Kriticos DJ, Makowski D, Pergl J, Reynaud P, Robinet C, Worner S (2012) Rating and mapping the suitability of the climate for pest risk analysis. EPPO Bull 42:48–55. https://doi.org/10.1111/j.1365-2338.2012.02549.x

Eyring V, Bony S, Meehl GA, Senior CA, Stevens B, Stouffer RJ, Taylor KE (2016) Overview of the Coupled Model Intercomparison Project Phase 6 (CMIP6) experimental design and organization. Geosci Model Dev 9:1937–1958. https://doi.org/10.5194/gmd-9-1937-2016

Hersbach H, Comyn Platt E, Bell B, Berrisford P, Biavati G, Horányi A, Muñoz Sabater J, Nicolas J, Peubey C, Radu R, Rozum I, Schepers D, Simmons A, Soci C, Dee D, Thépaut JN, Cagnazzo C, Cucchi M (2023) ERA5 post-processed daily statistics on pressure levels from 1940 to present. Copernicus Climate Change Service (C3S) Climate Data Store. https://doi.org/10.24381/cds.4991cf48

Hochmaier V (2014) Chilling unit accumulation and degree-day requirements of four sweet cherry (*Prunus avium* L.) cultivars. Acta Hortic 1020:203–207. https://doi.org/10.17660/ActaHortic.2014.1020.29

Hoffmann EJ, Coombs AB, Whalon ME (2004) Reproductive development of northern and southern strains of plum curculio (Coleoptera: Curculionidae). J Econ Entomol 97:27–32. https://doi.org/10.1093/jee/97.1.27

Kriticos DJ, Maywald GF, Yonow T, Zurcher EJ, Herrmann NI, Sutherst RW (2015) CLIMEX Version 4: exploring the effects of climate on plants, animals and diseases. CSIRO, Canberra

877 Kriticos D, Szyniszewska A, Bradshaw C, Li C, Verykouki E, Yonow T et al (2024) Modelling tools for
878 including climate change in pest risk assessments. EPPO Bull 54:38–51. https://doi.org/10.1111/epp.12994
879
880 Lampasona TP, Rodriguez Saona C, Leskey TC, Nielsen AL (2020) A review of the biology, ecology, and
881 management of plum curculio (Coleoptera: Curculionidae). J Integr Pest Manag 11:22.
882 https://doi.org/10.1093/jipm/pmaa018
883
884 Lan Z, Scherm H, Horton DL (2004) Temperature-dependent development and prediction of emergence of
885 the summer generation of plum curculio (Coleoptera: Curculionidae) in the southeastern United States.
886 Environ Entomol 33:174–181. https://doi.org/10.1603/0046-225X-33.2.174
887
888 Leskey TC (2008) Reproductive development of female plum curculio (Coleoptera: Curculionidae) in the
889 Mid-Atlantic: presence of multivoltine populations. J Entomol Sci 43:208–216.
890 https://doi.org/10.18474/0749-8004-43.2.208
891
892 Leskey TC, Zhang A (2007) Impact of temperature on plum curculio (Coleoptera: Curculionidae) responses
893 to odor-baited traps. J Econ Entomol 100:343–349. https://doi.org/10.1093/jee/100.2.343
894
895 Magarey RD, Borchert DM, Engle JS, Colunga Garcia M, Koch FH, Yemshanov D (2011) Risk maps for
896 targeting exotic plant pest detection programs in the United States. EPPO Bull 41:46–56.
897 https://doi.org/10.1111/j.1365-2338.2011.02437.x
898
899 McGiffen ME, Meyer JR, Boyne JV (1987) Physiological parameters of diapause and reproduction in the
900 plum curculio, *Conotrachelus nenuphar* (Herbst) (Coleoptera: Curculionidae). Ann Entomol Soc Am
901 80:284–287. https://doi.org/10.1093/aesa/80.2.284
902
903 Meier U (2018) Growth stages of mono- and dicotyledonous plants: BBCH monograph. Open Agrar
904 Repositorium, Quedlinburg. https://doi.org/10.5073/20180906-074619
905
906 Meinshausen M, Nicholls ZRJ, Lewis J, Gidden MJ, Vogel E, Freund M et al (2020) The shared socio-
907 economic pathway (SSP) greenhouse gas concentrations and their extensions to 2500. Geosci Model Dev
908 13:3571–3605. https://doi.org/10.5194/gmd-13-3571-2020
909
910 O'Neill BC, Tebaldi C, van Vuuren DP, Eyring V, Friedlingstein P, Hurtt G et al (2016) The Scenario Model
911 Intercomparison Project (ScenarioMIP) for CMIP6. Geosci Model Dev 9:3461–3482.
912 https://doi.org/10.5194/gmd-9-3461-2016
913

Parding KM, Dobler A, McSweeney CF, Landgren OA, Benestad R, Erlandsen HB et al (2020) GCMeval—an interactive tool for evaluation and selection of climate model ensembles. Clim Serv 18:100167. https://doi.org/10.1016/j.cliser.2020.100167

Pereira FP, Diniz AJF, Parra JRP (2023) Fertility life table, thermal requirements, and ecological zoning of Anthonomus grandis grandis Boheman (Coleoptera: Curculionidae) in Brazil. Insects 14:582. https://doi.org/10.3390/insects14070582

PEP725 Pan European Phenology Data (2026) Pan European Phenology Data. https://www.pep725.eu/. Accessed 16 February 2026

Piñero JC, Prokopy RJ (2006) Temporal dynamics of plum curculio, Conotrachelus nenuphar (Herbst) (Coleoptera: Curculionidae), immigration into an apple orchard in Massachusetts. Environ Entomol 35:413–422. https://doi.org/10.1603/0046-225X-35.2.413

Quaintance AL, Jenne EL (1912) The plum curculio. Bulletin of the US Department of Agriculture, Bureau of Entomology 103:1–250

R Core Team (2024) R: a language and environment for statistical computing. R Foundation for Statistical Computing, Vienna. http://www.R-project.org/

Racette G, Chouinard G, Vincent C, Hill SB (1992) Ecology and management of plum curculio, Conotrachelus nenuphar (Coleoptera: Curculionidae), in apple orchards. Phytoprotection 73:85–100. https://doi.org/10.7202/706025ar

Reissig WH, Nyrop JP, Straub R (1998) Oviposition model for timing insecticide sprays against plum curculio (Coleoptera: Curculionidae) in New York State. Environ Entomol 27:1053–1061. https://doi.org/10.1093/ee/27.5.1053

Rosace MC, Björklund N, Boberg J, Bradshaw CD, Camac J, Damus M et al (2024) Including climate change in pest risk assessment: current practices and perspectives for future implementation. EPPO Bull 54:52–72. https://doi.org/10.1111/epp.12989

Selby RD, Whalon ME (2014) Comparing the emergence of northern strain plum curculio larvae from multiple fruit varieties. J Econ Entomol 107:1543–1553. https://doi.org/10.1603/EC14180

Singh M, Bhatia HS (2011) Thermal time requirements for phenophases of apple genotypes in Kullu valley. J Agrometeorol 13:46–49. https://doi.org/10.54386/jam.v13i1.1333

Smith EH, Salkeld EH (1964) Ovary development and oviposition rates in the plum curculio, Conotrachelus nenuphar (Coleoptera: Curculionidae). Ann Entomol Soc Am 57:781–787. https://doi.org/10.1093/aesa/57.6.781

Spurgeon DW, Raulston JR (2006) Boll weevil (Coleoptera: Curculionidae) adult diapause responses to selected environmental and dietary conditions. Ann Entomol Soc Am 99:1085–1100. https://doi.org/10.1603/0013-8746(2006)99[1085:BWCCAD]2.0.CO;2

Spurgeon DW, Suh CPC, Esquivel JF (2018) Diapause response of the boll weevil (Coleoptera: Curculionidae) to feeding period duration and cotton square size. J Insect Sci 18:1. https://doi.org/10.1093/jisesa/iey084

Templ B, Koch E, Bolmgren K, Ungersböck M, Paul A, Scheifinger H et al (2018) Pan-European phenological database (PEP725): a single point of access for European data. Int J Biometeorol 62:1109–1113. https://doi.org/10.1007/s00484-018-1512-8

Tuomola J (2025) Assessment of the likelihood of establishment of Aromia bungii in Finland based on availability of host plants and suitability of climate. Finnish Food Authority, Research Reports 2/2025. http://hdl.handle.net/10138/599457

Tuomola J, Gruffudd H, Ruosteenoja K, Hannunen S (2021) Could pine wood nematode, *Bursaphelenchus xylophilus*, cause pine wilt disease or establish inside healthy trees in Finland now—or ever? Forests 12:1679. https://doi.org/10.3390/f12121679

Tuomola J, Hannunen S (2024) Assessment of the suitability of the Finnish climate for *Popillia japonica*. Finnish Food Authority, Research Reports 3/2024. http://hdl.handle.net/10138/570090

Venette RC, Kriticos DJ, Magarey RD, Koch FH, Baker RHA, Worner SP et al (2010) Pest risk maps for invasive alien species: a roadmap for improvement. BioScience 60:349–362. https://doi.org/10.1525/bio.2010.60.5.5

Verma P, Singh J, Sharma S, Thakur H (2023) Phenological growth stages and growing degree days of peach, Prunus persica (L.) Batsch, in a sub-temperate Himalayan region using BBCH scale. Ann Appl Biol 182:284–294. https://doi.org/10.1111/aab.12815

Wakie TT, Yee WL, Neven LG (2018) Assessing the risk of establishment of *Rhagoletis cerasi* (Diptera: Tephritidae) in the United States and globally. J Econ Entomol 111:1275–1284. https://doi.org/10.1093/jee/toy054

Whitcomb WD (1929) The plum curculio in apples in Massachusetts. Massachusetts Agricultural Experiment Station Bulletin 249:26–52

Whitcomb WD (1932) The relation of temperature to the activity and control of the plum curculio in apples. Massachusetts Agricultural Experiment Station Bulletin 285:1–16

Zavalloni C, Andresen JA, Flore JA (2006) Phenological models of flower bud stages and fruit growth of 'Montmorency' sour cherry based on growing degree-day accumulation. J Am Soc Hortic Sci 131:601–607. https://doi.org/10.21273/JASHS.131.5.601

Zhang X, Tu Z, Luckhart S, Pfeiffer DG (2008) Genetic diversity of plum curculio (Coleoptera: Curculionidae) among geographical populations in the eastern United States. Ann Entomol Soc Am 101:824–832. https://doi.org/10.1603/0013-8746(2008)101[824:GDOPCC]2.0.CO;2

Statements & Declarations

Data availability statement

The full R script used to define the distributions and perform the simulations, as well as the simulation results that support the findings of this study, are available at Zenodo: https://doi.org/10.5281/zenodo.20541446. The archived outputs are derived products generated from ERA5 and CMIP6 climate data and PEP725 phenological observations. The original third-party input data are not redistributed. ERA5 and CMIP6 climate data used in this study were obtained from the Climate Data Store (CDS) of the Copernicus Climate Change Service (C3S). CMIP6 model output is also available through the Earth System Grid Federation (ESGF), and PEP725 phenological observations are available from the Pan European Phenological Database. Users wishing to reproduce the full workflow should obtain the original input data from the respective providers and comply with their citation, acknowledgement and license requirements. This study contains modified Copernicus Climate Change Service information 2026. Neither the European Commission nor ECMWF is responsible for any use that may be made of the Copernicus information or data it contains.

Funding

This research was part of the Postdoctoral Programme for Research Institutes in Finland funded by the Finnish Government.

Competing Interests

The authors have no relevant financial or non-financial interests to disclose.

Author Contributions

JT conceived and designed the study, performed the modelling work, and drafted the first version of the manuscript. MM-T, SL and LO contributed to the conception and development of the modelling design and collected additional data and information used to refine the modelling. All authors contributed to the revision of the manuscript, provided critical intellectual input, and approved the final version for publication.